Published OnlineFirst January 25, 2011; DOI:10.1158/1078-0432.CCR-10-1859

Clinical Cancer Research

A20, *ABIN-1/2*, and *CARD11* Mutations and Their Prognostic Value in Gastrointestinal Diffuse Large B-Cell Lymphoma

Gehong Dong, Estelle Chanudet, Naiyan Zeng, et al.

Clin Cancer Res 2011;17:1440-1451. Published OnlineFirst January 25, 2011.

Published OnlineFirst January 25, 2011; DOI:10.1158/1078-0432.CCR-10-1859

Clinical Cancer Research

Imaging, Diagnosis, Prognosis

A20, *ABIN-1/2*, and *CARD11* Mutations and Their Prognostic Value in Gastrointestinal Diffuse Large B-Cell Lymphoma

Gehong Dong[1,2], Estelle Chanudet[1], Naiyan Zeng[1], Alex Appert[1], Yun-Wen Chen[3], Wing-Yan Au[4], Rifat A. Hamoudi[1], A. James Watkins[1], Hongtao Ye[1], Hongxiang Liu[1], Zifen Gao[2], Shih-Sung Chuang[5], Gopesh Srivastava[3], and Ming-Qing Du[1]

Abstract

Purpose: Diffuse large B-cell lymphoma (DLBCL) is a heterogeneous group of aggressive lymphomas with the activated B-cell–like subtype characterized by constitutive NF-κB activation. Activating mutations of *CARD11* and inactivating mutations of *A20* are frequent events in DLBCL. However, the full extent of genetic alterations in the NF-κB pathway regulators and their potential prognostic value in DLBCL remain to be investigated. We investigated the genetic abnormalities of *CARD11*, *A20*, and *ABIN-1/2/3* (the A20 binding inhibitor of NF-κB) and their clinicopathologic correlation in gastrointestinal DLBCL.

Experimental Design: The somatic mutation and copy number changes of *CARD11*, *A20*, and *ABIN-1/2/3* were investigated in 71 gastrointestinal DLBCLs by PCR/sequencing, and interphase FISH/array comparative genomic hybridization, respectively. The mutations identified were functionally characterized by NF-κB reporter assays and immunoprecipitation experiments.

Results: Recurrent somatic mutations were found in *CARD11* (10%), *A20* (17%), *ABIN-1* (4%), and *ABIN-2* (3%), but not in *ABIN-3*. In comparison with the wild-type, all CARD11 mutants were potent NF-κB activators *in vitro*. On the basis of the destructive nature of the observed mutations, and the findings by reporter assays and immunoprecipitation studies, most if not all of the somatic mutations that were seen in *A20*, *ABIN-1*, and *ABIN-2* could impair their normal functions. Among these genetic abnormalities, *A20* somatic mutation was significantly associated with both poor overall survival and event-free survival.

Conclusions: We show further evidence of NF-κB pathway genetic abnormalities in DLBCL, which are potentially valuable in the prognosis and design of future therapeutic strategies. *Clin Cancer Res; 17(6); 1440–51. ©2011 AACR.*

Introduction

NF-κB is a master transcription factor that is critical to a number of biological processes that are involved in both innate and adaptive immunity. There is growing evidence that NF-κB is constitutively activated in several lymphoma subtypes, including MALT lymphoma (1), activated B-cell–like diffuse large B-cell lymphoma (ABC-DLBCL; refs. 2, 3), primary mediastinal large B-cell lymphoma (PMBL; refs. (4, 5), and multiple myeloma (MM; ref. 6), and NF-κB activity is essential to the survival of these lymphoma cells (7). The genetic bases that underlie the constitutive NF-κB activation in these lymphomas have received extensive investigation (8–11). The two most recent exciting advances in this field of research concern the findings of CARD11 activation and A20 inactivation in several lymphoma subtypes.

CARD11, which is also known as CARMA1 (CARD-MAGUK protein 1), is a scaffolding molecule that links antigen receptor signaling to the BCL10/MALT1-mediated NF-κB activation (12). Using an unbiased loss-of-function RNA interference screen, Ngo and colleagues have shown that CARD11 was critical for the proliferation and survival of ABC-DLBCL cells but not germinal center B-cell like (GCB) DLBCL cells (13). Subsequent mutational analysis by Lenz and colleagues identified missense mutations in 7 of 73 (9.6%) ABC-DLBCL and 3 of 79 (3.8%) GCB-DLBCL, and all of the *CARD11* mutations were within the coiled-coil domain and were capable of activating the NF-κB reporter gene *in vitro* (14). Two recent studies confirmed similar frequencies of *CARD11* mutation in nodal DLBCL (15, 16).

Authors' Affiliations: [1]Division of Molecular Histopathology, Department of Pathology, University of Cambridge, Cambridge, United Kingdom; [2]Department of Pathology, Health Science Centre, Beijing University, Beijing, China; Departments of [3]Pathology and [4]Medicine, The University of Hong Kong, Queen Mary Hospital, Hong Kong, China; and [5]Department of Pathology, Chi-Mei Medical Centre, Tainan and Taipei Medical University, Taipei, Taiwan

Note: Supplementary data for this article are available at Clinical Cancer Research Online (http://clincancerres.aacrjournals.org/).

Note: G. Dong, E. Chanudet, and N. Zeng contributed equally to this article.

Corresponding Author: Ming-Qing Du, Division of Molecular Histopathology, Department of Pathology, University of Cambridge, Level 3 Lab Block, Box 231, Addenbrooke's Hospital, Hills Road, Cambridge, CB2 0QQ, United Kingdom. Phone: 44-01223-767092; Fax: 44-01223-586670. Email: mqd20@cam.ac.uk

doi: 10.1158/1078-0432.CCR-10-1859

Published OnlineFirst January 25, 2011; DOI:10.1158/1078-0432.CCR-10-1859

Translational Relevance

Diffuse large B-cell lymphoma (DLBCL) shows variable clinical outcome with the activated B-cell subtype characterized by constitutive NF-κB activation and poor prognosis. The genetic bases for the constitutive NF-κB activation in DLBCL remain largely unknown, nor the value of such genetic abnormalities in DLBCL diagnosis and treatment prediction. We report several important novel observations on genetic abnormalities of NF-κB regulators in DLBCL and specifically we showed:

(1) *ABIN-1* and *ABIN-2*, the adaptors of the A20 inhibitory complex of the NF-κB activation pathway, were also recurrently targeted by inactivating somatic mutations;

(2) *A20*, *ABIN-1*, *ABIN-2*, and *CARD11* somatic mutation were almost mutually exclusive;

(3) *A20* somatic mutation was significantly and independently associated with both poor overall survival and event-free survival.

These findings provide further evidence of NF-κB pathway genetic abnormalities in DLBCL, which are potentially valuable in prognosis and design of future therapeutic strategy.

A20, which is also known as TNFα-induced protein 3 (*TNFAIP3*), is a "global" essential negative regulator of the NF-κB activation pathway and can attenuate the NF-κB activity that is triggered by signaling from TNF and Toll-like receptors (17–19). By array comparative genomic hybridization (CGH), we and others have identified *A20* as the target of a 6q23 deletion in ocular adnexal MALT lymphoma (8, 20, 21). By interphase FISH, we have shown that *A20* deletion, which frequently involves both alleles, preferentially occurs in translocation-negative MALT lymphoma of the ocular adnexa (19%), salivary gland (8%), and thyroid (11%), but not in those of the lung and stomach (8). Several independent studies have further shown the frequent inactivation of *A20* by mutation and/or deletion in MALT lymphoma (18–22%), DLBCL (7.8%–54%), Hodgkin's lymphoma (33%–44%), and PMBL lymphoma (36%; refs. 15, 16, 22–24). In a recent study, we found that a *A20* hemizygous deletion was commonly associated with its promoter methylation and that complete inactivation of the *A20* gene by deletion/promoter methylation or biallelic deletion is significantly associated with a poor lymphoma-free survival in ocular adnexal MALT lymphoma (9).

Despite the aforementioned exciting advances, several imperative questions remain to be answered. Are A20 inactivation and CARD11 activation mutually exclusive? A20 requires its binding partner, such as *ABIN-1/2/3* (the A20 binding inhibitor of NF-κB), to function as a negative regulator of the NF-κB activation pathway (25). Are these A20 adaptor molecules also targeted by genetic abnormalities in lymphoma? What are the clinical impacts of these NF-κB regulator abnormalities, and can these abnormalities be used as a prognostic marker? To address these questions, we have comprehensively investigated the genetic abnormalities of *CARD11*, *A20*, and *ABIN-1/2/3* (the A20 binding inhibitor of NF-κB) in gastrointestinal DLBCL, which is poorly understood at the genetic level although the majority of gastric DLBCL are associated with *Helicobacter pylori* infection and the response of gastrointestinal DLBCL to treatment is much favorable than nodal DLBCL (26–28). Comprehensive correlations among the genetic abnormalities were identified and clinicopathologic parameters were performed.

Materials and Methods

Tissue materials

A total of 71 cases of primary gastrointestinal DLBCL (43 gastric, 28 intestinal) from the authors' institutions were successfully investigated in this study. Among these cases, a low-grade MALT lymphoma component was identified in 13 cases (18%). Thirty-nine cases had both frozen and formalin-fixed paraffin-embedded (FFPE) tissue specimens, whereas the remaining 32 cases had only FFPE tissues. The clinicopathologic features of the majority of these cases have been described elsewhere (29, 30). Local ethical guidelines were followed for the use of archival tissues for research with the approval of the ethics committees of the involved institutions.

Immunohistochemistry

This was carried out routinely on FFPE tissue sections with streptavidin-biotin peroxidase method by using mouse monoclonal antibodies. Classification of DLBCL into germinal center (GC) and non-GC subgroups was based on immunohistochemical analysis of CD10 (Novocastra), and BCL6 and MUM1 (Dako) according to the algorithm of Hans and colleagues (31). For each antibody, cases were considered positive if 30% of DLBCL cells showed positive staining.

Microdissection and DNA preparation

Crude microdissection was done in each case to enrich tumor cells (32). DNA was extracted by using standard proteinase K digestion, followed by phenol/chloroform/isoamyl-alcohol extraction or by using the QIAamp DNA Micro Kit (QIAGEN). The quality of the DNA samples was assessed by the PCR amplification of variably sized gene fragments (33), and those with successful amplifications of genomic fragments in excess of 300 bp, in addition to the DNA samples from the frozen tissues, were used for mutational screening.

High-resolution melting analysis

High-resolution melting analysis (HRM) was used initially for the *CARD11* mutation screening. Fourteen primer sets were designed to amplify the coiled-coil domain of *CARD11*, which is encoded by exons 5 to 10, within which activating mutations were found in

Published OnlineFirst January 25, 2011; DOI:10.1158/1078-0432.CCR-10-1859

a previous study (14). The primer sequences and PCR conditions are detailed in Supplementary Table S1. HRM was performed immediately after PCR by the Rotor-Gene 6000 analyzer (Corbett Life Science). PCR samples with possible mutations were further investigated by direct DNA sequencing.

PCR and sequencing

In subsequent study, *CARD11* mutations were screened by PCR and direct sequencing because this was much efficient. In all cases, mutations in the *A20*, *ABIN-1*, *ABIN-2*, and *ABIN-3* genes were screened by PCR followed by sequencing. The primer sequence and PCR conditions are detailed in Supplementary Table S1. PCR products were routinely purified and directly sequenced in both orientations by using the BigDye terminator chemistry 3.1 system (Applied Biosystems). In each case, the presence of a mutation was confirmed by at least 2 independent PCR and sequencing experiments, and each mutation was verified as not being a polymorphism by a search of online NCBI and Ensemble databases and from a germline mutation by an analysis of DNA samples that had been prepared from normal tissues or microdissected normal cells.

Interphase fluorescence *in situ* hybridization

A20 (6q23) and TNFA/B/C (6p21) loci copy number changes were investigated by using a 3-color FISH assay as described in our previous study (8). Chromosome translocations involving the *BCL2*, *BCL6*, *CCND1*, *MYC*, and *IGH* loci were investigated by using respective dual-color break-apart probes and appropriate dual-color dual-fusion probes, where indicated (Vysis/Abbott Laboratories; ref. 34).

A20 promoter methylation analysis

DNA samples (600 ng) were converted by bisulfite treatment by using the EZ DNA methylation kit (Zymo Research). Two separate bisulfite treatments were preformed in each case so as to facilitate independent pyrosequencing experiments. One fifth of the converted DNA was PCR-amplified for a 222-bp fragment of the *A20* promoter that is upstream from the first exon (9). The PCR products were checked for specificity on 3% agarose gels and subjected to pyrosequencing by using Pyro Gold SQA reagents (Biotage) on a PyroMark MD pyrosequencer (Q-CPG software version 1.0.9, Biotage) as previously described (9).

NF-κB reporter assay

The full-length coding sequence of *CARD11*, *ABIN-1*, and *ABIN-2* was cloned into a modified pIRESpuro2 expression vector (Clontech), and various mutants of *CARD11*, *ABIN-1*, and *ABIN-2* were generated by using the QuickChange II XL site-directed mutagenesis kit (Stratagene). The capacity of these mutants to induce or suppress NF-κB activation was measured in Jurkat T cells and HEK293 cells by using a dual-luciferase reporter assay system (Promega; ref. 35). Briefly, Jurkat T cells (5×10^6) were transfected with 2 μg of expression vector, 0.8 μg of pNF-κB-luc (a firefly luciferase reporter for NF-κB activity), and 0.6 μg of pRL-TK (a Renilla luciferase reporter as a control) by using Amaxa nucleofector system (Amaxa). The transfected cells were cultured for 24 hours and then harvested for a luciferase assay. Similarly, HEK293 cells were transfected by Lipofectamine 2000 (Invitrogen), cultured for 22 hours, stimulated with TNFα (300 IU/mL) for 2 hours, and then harvested for luciferase activity measurement. For each experiment, at least 3 independent transfections and duplicate reporter assays were performed, and the data were normalized to appropriate controls and presented as a mean ± SD.

Immunoprecipitation

HEK293 cells were cotransfected with HA-A20 and Flag-ABIN-2 (wild-type or mutant) by using Lipofectamine 2000 and then collected for immunoprecipitation 24 hours later. Cells that were similarly transfected with an empty vector were used as a control. Immunoprecipitation of HA-A20 and Flag-ABIN-2 were performed by using the anti-HA immunoprecipitation kit and the Flag-tagged protein immunoprecipitation kit (Sigma-Aldrich), respectively, according to the manufacturer's instructions. Total cell lysate (input), flow-through, and immunoprecipitation eluate were analyzed by Western blot. The A20 binding capacity was calculated by quantifying the chemiluminescent signals of ABIN-2 and A20 proteins that were detected in the immunoprecipitation eluate by using the Quantity One software package (BioRad). For immunoprecipitation with HA-A20, the difference between the wild-type and mutant ABIN-2 that coimmunoprecipitated with A20 were compared after normalization by the amount of A20 in the eluate and vice versa for immunoprecipitation with Flag-ABIN-2. The immunoprecipitation experiments were conducted twice.

Statistical analysis

Overall survival (OS) was measured from the date of diagnosis to death from any cause. Event-free survival (EFS) was measured from the date of diagnosis to disease progression, relapse, or death from any cause. Probabilities of OS and EFS were calculated by the Kaplan–Meier method, and the comparison between subgroups was carried out via the log-rank test, wherein any variable that showed $P \leq 0.1$ was further tested by a multivariate analysis by using the Cox proportional hazard regression model. The correlation among variables was evaluated by Fisher's exact probability test. All statistical analyses were carried out by SPSS, version 13.

Results

CARD11, *A20*, and *ABIN-1/2/3* genetic abnormalities in gastrointestinal DLBCL

Of the 60 cases of gastrointestinal DLBCL that were analyzed by 1 Mb resolution CGH, 9 (15%) exhibited an extra copy of 7p22 that contained *CARD11*, whereas

Published OnlineFirst January 25, 2011; DOI:10.1158/1078-0432.CCR-10-1859

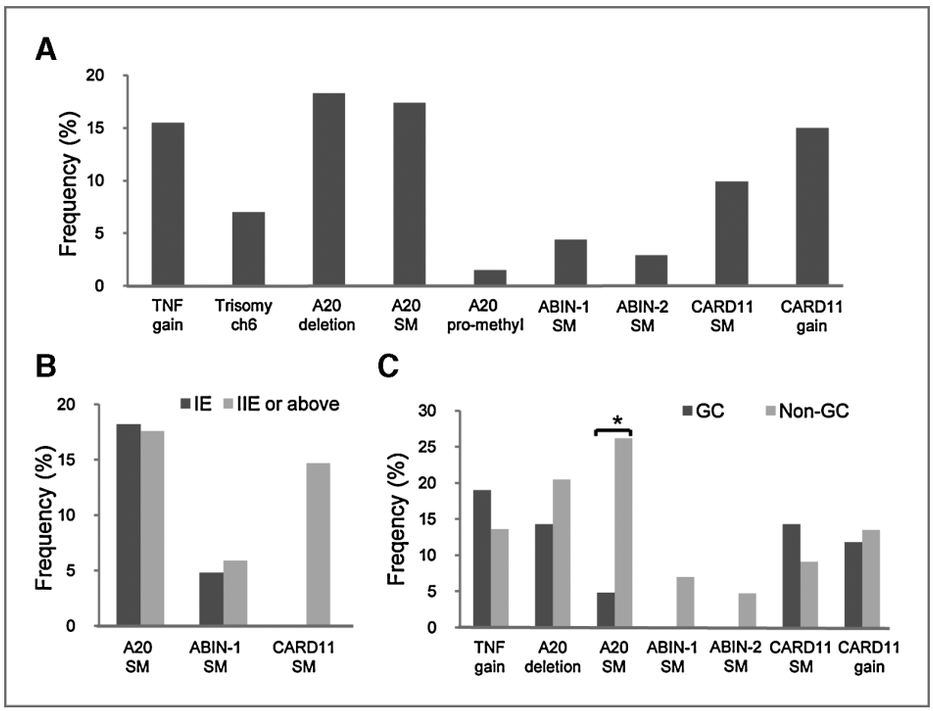

Figure 1. The frequencies of genetic abnormalities in gastrointestinal DLBCL and their correlation with clinical stage and immunophenotype. Gain of the *TNF* locus, deletion of the *A20* locus and somatic mutation (SM) of the *A20* and *CARD11* gene are a frequent event, whereas *A20* promoter methylation (pro-methyl) and SM of the *ABIN-1* and *ABIN-2* gene are relatively infrequent (A). *CARD11* SM is more frequently seen in cases with advanced stages, whereas *A20* and *ABIN-1* SMs show no association with clinical stage (B). Of the 4 genes investigated, only *A20* SM is significantly associated with non-GC immunophenotype (C). Germline mutation was also found in *A20*, *ABIN-1* and *ABIN2*, but not included in this figure. * $P < 0.05$.

none exhibited an amplification of this genomic locus (data not shown). A total of 71 cases of gastrointestinal DLBCL were investigated for mutations in the *CARD11* coiled-coil domain by a combination of HRM and sequencing (39 cases), direct sequencing (32 cases), or both methods (7 cases). A total of 9 mutations excluding known polymorphisms were identified in 7 cases, and a single case was observed to harbor 3 mutations (G126D, V266D, and T353P; Figs. 1A and 2A; Supplementary Table S2). Because there was no frozen tissue available, it was not possible to amplify the genomic or cDNA sequence that included all the 3 mutation sites to investigate whether these different mutations occurred in one or both alleles of the *CARD11* gene. The somatic origin of these mutations was confirmed in each of the 6 cases where DNA samples had been successfully extracted from the microdissected normal cells. In the remaining case, it was not possible to microdissect enough normal cells; however, the mutant was much more potent than the wild-type in NF-κB activation (please see the following section), and, therefore, it was most likely pathogenic. The distribution of *CARD11* mutations that was observed in this study is similar to those that have been recently reported. These mutations seem to be clustered into 4 regions, and the only recurrent mutation has been observed in codon 126 (2 of 27 = 7%; Fig. 2A; refs. 14, 15).

Interphase FISH showed a heterozygous deletion of *A20* and a gain of the *TNFA/B/C* locus in 13 of 71 (18.3%) and 11 of 71 (15.5%) gastrointestinal DLBCL, respectively (Fig. 1A). There was no association between *A20* deletion and *TNFA/B/C* gain. PCR analysis of all *A20*-coding exons followed by DNA sequencing identified a total of 15 mutations, excluding known polymorphisms, in 13 of 69 (19%) cases, wherein 2 cases were each observed to harbor 2 mutations (one case exhibited a 77-bp deletion and a M476I mutation in exon 7, whereas the other displayed a 6-bp deletion in exon 2 and a 1-bp deletion in exon 6; ref. Fig. 1A; Supplementary Table S2). Because there was no frozen tissue, it was not possible to investigate whether these mutations occurred in one or both alleles of the *A20* gene. PCR and sequence analyses of the DNA samples that had been extracted from microdissected normal cells confirmed the somatic origin of the detected mutations in 12 of 13 cases, whereas the remaining case exhibited a germline missense mutation (Supplementary Table S2). There was no association between *A20* deletion and mutation. Pyrosequencing showed evidence of promoter methylation in 1 of 69 (1.4%) cases (Supplementary Figs. S1A and S2), and this single case did not display an *A20* deletion or mutation.

Among the 14 *A20* somatic mutations that were identified in this study, the majority (79%) were predicted to produce truncated proteins due to out-frame insertion (2 cases) or deletion (6 cases), nonsense mutation (1 case), or mutation in the splicing site (2 cases), whereas the remaining 3 mutations (21%) were missense mutations (Fig. 2B). These mutations are similar in nature to those that have been recently reported (Fig. 2B), and they would most likely impair A20 function (15, 16, 22–24). Nonetheless, unlike these reported mutations, the mutations that were observed in gastrointestinal DLBCL were biased toward the ovarian tumor (OTU) domain, which belongs to the family of deubiquitinating cysteine proteases (Fig. 2B).

Published OnlineFirst January 25, 2011; DOI:10.1158/1078-0432.CCR-10-1859

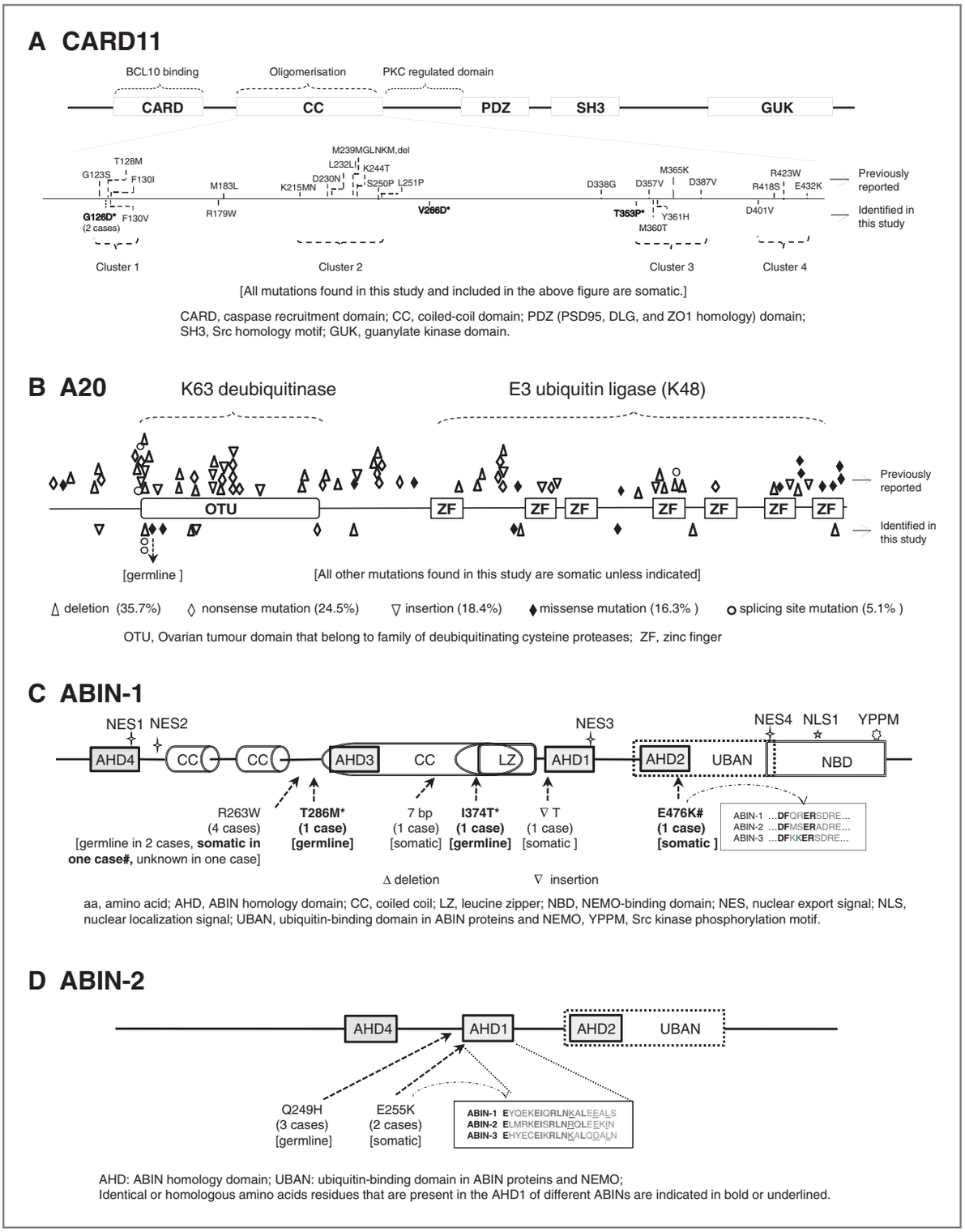

Figure 2. The distribution of mutations in *CARD11*, *A20*, *ABIN-1*, and *ABIN-2* in gastrointestinal DLBCL. Multiple mutations that occur in the same gene in the same case are indicated by * or # in bold. *CARD11* mutations are exclusively somatic missense changes that gain capacity to activate NF-κB. Majority of *A20* somatic mutations seen in gastrointestinal DLBCL are destructive changes (frameshift and nonsense mutations), similar to those reported in other lymphoma subtypes. *ABIN-1* somatic mutations are composed of frameshift changes and missense mutations, and the latter often occurs at the conserved amino acid residuals. Two recurrent *ABIN-2* mutations are seen in gastrointestinal DLBCL and the somatic mutation (E255K) occurs at the conserved amino acid residual.

Published OnlineFirst January 25, 2011; DOI:10.1158/1078-0432.CCR-10-1859

A20 requires its binding partner, that is, adaptor proteins, to function as a negative regulator of the NF-κB activation pathway, and ABIN-1/2/3 are its major adaptor molecules. We next investigated *ABIN* genetic abnormalities. None of the 60 cases of gastrointestinal DLBCL that were analyzed by 1 Mb resolution array CGH exhibited evidence of deletion at the *ABIN-1* (5q32-33.1), *ABIN-2* (4p16.3), or *ABIN-3* (4q27) loci (data not shown). PCR and sequencing of all of the *ABIN-1*–coding exons identified a total of 9 mutations, excluding known polymorphisms, in 7 of 68 (10.3%) cases (Fig. 2C; Supplementary Table S2). Two cases each harbored 2 mutations (one showed somatic R263W and E476K in exons 8 and 14, respectively, whereas the other displayed germline T286M and I374T in exons 9 and 11, respectively). Another 2 cases exhibited somatic insertions or deletions that caused a reading frameshift, and the predicted truncated products lack important functional domains, including AHD1 (ABIN homology domain), AHD2, UBAN (ubiquitin binding domain in ABIN and NEMO), and NBD (NEMO binding domain). The remaining 3 cases each displayed a recurrent missense mutation (R263W) that was downstream of the second coiled-coil domain, which was confirmed to be a germline alteration in 2 cases, in which normal DNA was available for analysis (Fig. 2C).

Similarly, PCR and sequencing of all *ABIN-2*–coding exons identified a total of 5 mutations, excluding known polymorphisms, in 5 of 68 (7.4%) cases (Fig. 1A). Two cases exhibited a recurrent somatic missense mutation at the conserved residue (E255) of AHD1, whereas the remaining 3 cases displayed a recurrent germline missense mutation at amino acid 249, which is immediately upstream of AHD1 (Fig. 2D). The AHD1 in ABIN-2 is critical to the binding of both A20 and NEMO (36), whereas the region (amino acids 194–250) that is upstream of AHD1 is responsible for the binding of TPL2 (37). Thus, these mutations may affect these protein–protein interactions and impair ABIN-2 function.

ABIN-3 contains 14 coding exons (including alternative spliced exons) and exons 8 to 10, which encode AHD1, 2, and 4 and the UBAN domain. The PCR analysis and sequencing of these 3 coding exons in the 40 cases of gastrointestinal DLBCL did not show any evidence of somatic mutation.

Interphase FISH was performed to investigate the chromosome translocations that are frequently seen in DLBCL and exhibited evidence of translocations involving the *BCL2* (2 of 51 cases), *BCL6* (10 of 48), and *MYC* (2 of 49) genes but not the *CCND1* gene (0 of 50; Supplementary Table S2).

Comprehensive correlation analyses showed that there was no association among these somatic mutations and chromosomal structural and numerical changes. *A20*, *ABIN-1*, *ABIN-2*, and *CARD 11* somatic mutations were almost mutually exclusive. Among the 21 cases with somatic mutation in any of these 4 genes, only 1 case exhibited concurrent mutations (Supplementary Table S2).

The functional impact of *ABIN-1*, *ABIN-2*, and *CARD11* mutations

To examine the functional consequence of *CARD11*, *ABIN-1*, and *ABIN-2* mutations, we first investigated whether the CARD11 mutants gained the ability to activate NF-κB and whether ABIN-1/2 mutants lose the ability to inhibit NF-κB activation via the use of a reporter assay.

In comparison with the wild-type, all 9 CARD11 mutants that were identified in this study were capable of activating the NF-κB reporter in Jurkat T cells in the absence of any immune receptor stimulation, and interestingly, these CARD11 mutants were much more potent than the BCL10, MALT1, and API2-MALT1 fusion products (Fig. 3A).

For *ABIN-1* mutation, we did not include the 2 frameshift mutations in the *in vitro* functional investigations. These mutations predicted truncated proteins that lacked the critical functional domains, including AHD1, UBAN, and NBD, and would certainly impair ABIN-1 function. All of the remaining ABIN-1 and ABIN-2 mutations were subjected to the NF-κB reporter assay. As expected, both wild-type ABIN-1 and ABIN-2 were capable of inhibiting CARD11- and TNFα-mediated NF-κB activation (Fig. 3B). Among the 4 *ABIN-1* missense mutations that were investigated, the E476K somatic mutant totally lost the ability to inhibit NF-κB activation, and the remaining 3 germline mutants exhibited no apparent difference from the wild-type. Among the 2 ABIN-2 missense mutations, both the E255K somatic mutant and the Q249H germline mutant were less efficient than the wild-type ABIN-2 in the inhibition of CARD11-mediated NF-κB activation in Jurkat T cells (Fig. 3C). Intriguingly, such inhibition was not seen in TNFα-mediated NF-κB activation in HEK293 cells (Fig. 3C).

To further investigate the ABIN-2 E255K mutant, we investigated its binding to A20 by coimmunoprecipitation. In comparison with the wild-type ABIN-2, the E255K mutant lost 70% of its A20 binding capacity (Fig. 3D).

A20 mutation was significantly associated with poor survival

Comprehensive correlation between the aforementioned genetic abnormalities and clinicopathologic parameters was performed. *A20* somatic mutation was significantly associated with the non-GC subtype of DLBCL (Fig. 1C; $P = 0.038$), as defined by the immunohistochemistry algorithm of Hans and colleagues (31). Such an association was not seen for *ABIN-1/2* and *CARD11* somatic mutations (Fig. 1B and C). Conversely, *CARD11* somatic mutations exhibited a strong trend of association with more advanced stages (>IIE or above) of DLBCL (Fig. 1B; $P = 0.066$).

Clinical follow-up data were available for 55 cases. The majority (32) of these cases were first treated with an anthracycline containing chemotherapy, for example, CEOP (cyclophosphamide, epirubicin, vincristine, and prednisone), CHOP (cyclophosphamide, doxorubicin,

Published OnlineFirst January 25, 2011; DOI:10.1158/1078-0432.CCR-10-1859

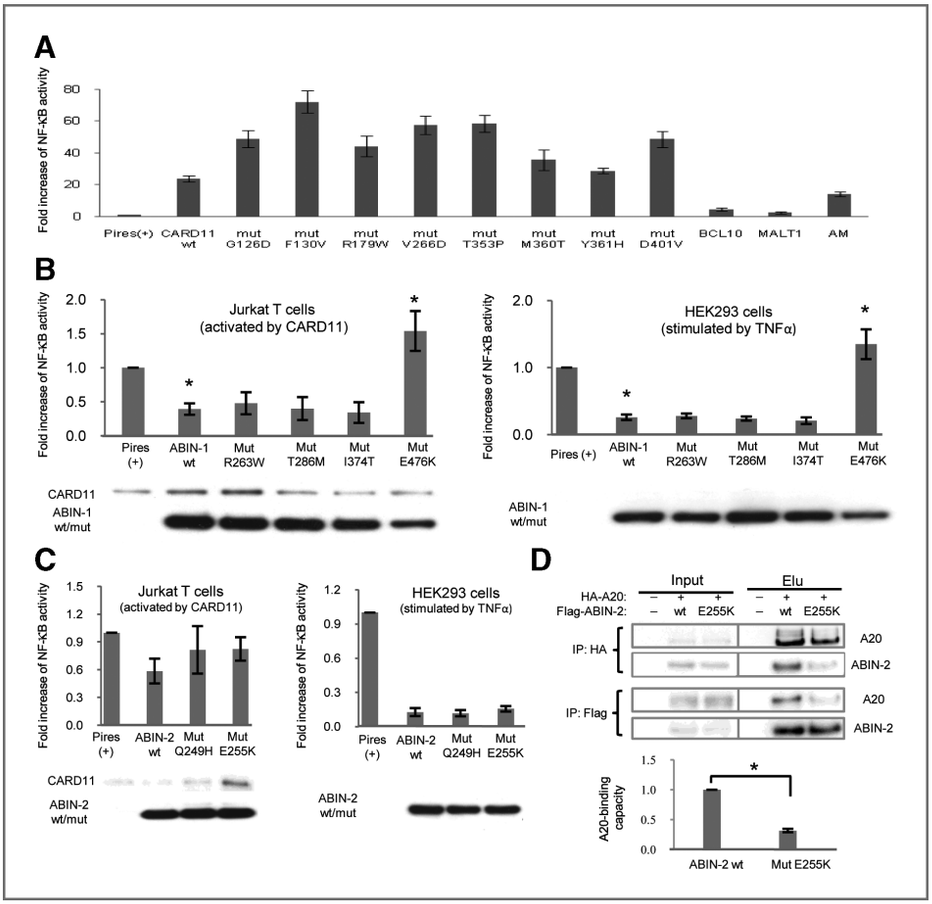

Figure 3. The functional characterization of *CARD11*, *ABIN-1*, and *ABIN-2* mutations. (A) all 8 CARD11 mutants (mut) that are seen in gastrointestinal DLBCL are much more potent than the wild-type (wt) CARD11 in NF-κB activation, as shown by the luciferase reporter assay in Jurkat T cells. (B) In comparison with the wild-type ABIN-1, the E476K somatic mutant does not inhibit NF-κB activation by CARD11 in Jurkat T cells and TNFα in HEK293 cells. In contrast, the 3 germline mutants (R263W, T286M, and I374T) show no apparent difference from the wild-type. (C) In comparison with the wild-type ABIN-2, the E255K somatic mutant and the Q249H germline mutant are less efficient in inhibiting NF-κB activation by CARD11 in Jurkat T cells; however, such an effect is not seen in TNFα-mediated NF-κB activation in HEK293 cells. (D) Coimmunoprecipitation shows that the ABIN-2 E255K mutant is impaired in its binding to A20 in comparison with its wild-type. The data that correspond to the NF-κB reporter assays represent 3 (Jurkat T cells) or 4 (HEK293 cells) independent experiments, whereas the coimmunoprecipitation (IP) experiment was performed twice. * $P < 0.01$. Pires(+): Vector control; AM: API2-MALT1.

vincristine, and prednisolone), and R-CHOP (rituximab-CHOP), with the remaining cases being treated with other therapy regimens, surgery alone, or surgery in combination with chemotherapy (Supplementary Table S2).

In light of the heterogeneous treatments, we focused our analyses on the cases treated with an anthracycline containing therapy. The clinical follow-up period in this group of patients ranged from 0 to 150.5 months (median 51.5 months) and the 5-year OS and EFS were 48.1% and 40.7%, respectively. Comprehensive correlation between the observed somatic genetic abnormalities and clinicopathologic parameters was carried out. The results of a univariate analysis of the prognostic variables are summarized in Table 1. Patients with advanced stages of disease exhibited a strong trend of association with both poor OS ($P = 0.063$) and EFS ($P = 0.043$). Among the *A20*, *ABIN-1*, and *CARD11* genetic abnormalities, the *A20* somatic mutations showed a significant association with both poor OS ($P = 0.001$) and EFS ($P = 0.002$; Table 1 and Figure 4). *CARD11* mutation also displayed a trend of association with poor EFS although not statistically significant ($P = 0.088$). There was no association between *A20* deletion, *ABIN-1* and *ABIN-2* somatic mutations, and patient survival. However, the number of cases with these genetic abnormalities was small for a reliable survival analysis. Multivariate analyses of the parameters that initially exhibited a trend of association with survival ($P \leq 0.1$) by univariate analysis showed that only the *A20* somatic mutation was an independent prognostic marker for both OS and EFS (Table 2).

Discussion

By screening the genetic abnormalities of NF-κB regulators in gastrointestinal DLBCL and correlating these abnormalities to clinicopathologic parameters, we have

Published OnlineFirst January 25, 2011; DOI:10.1158/1078-0432.CCR-10-1859

Table 1. The results of the univariate analysis for prognosis, as evaluated by the Kaplan–Meier method

Factors	*n*	OS		EFS	
		5 y	*P*[a]	5 y	*P*[a]
Age (year)					
<59	17	0.588	0.250	0.588	0.198
≥60	15	0.503		0.367	
Sex					
Female	14	0.643	0.371	0.571	0.477
Male	18	0.476		0.421	
Clinical stage					
IE	11	0.700	0.063	0.716	**0.043**
≥IIE	20	0.450		0.350	
CD10 expression					
Positive	8	0.750	0.157	0.625	0.195
Negative	22	0.431		0.390	
BCL6 expression					
Positive	20	0.633	**0.035**	0.584	**0.042**
Negative	10	0.300		0.200	
MUM1 expression					
Positive	20	0.424	0.419	0.379	0.412
Negative	9	0.667		0.556	
Immunophenotype by the Hans and colleagues algorithm (31)					
GC	10	0.700	0.184	0.600	0.270
Non-GC	20	0.424		0.379	
CARD11 somatic mutation[b]					
Positive	3	0.667	0.319	0.333	0.088
Negative	23	0.652		0.609	
A20 somatic mutation					
Positive	6	0.000	**0.001**	0.000	**0.002**
Negative	26	0.654		0.577	
A20 deletion[b]					
Positive	3	0.667	0.438	0.333	0.336
Negative	23	0.625		0.609	
ABIN-1 somatic mutation[b]					
Positive	2	0.500	0.727	0.500	0.755
Negative	22	0.636		0.545	
BCL6-involved translocation[b]					
Positive	1	0.000	0.134	0.000	0.405
Negative	25	0.680		0.600	
Any chromosome translocation[b,c]					
Positive	5	0.600	0.684	0.600	0.983
Negative	8	0.750		0.625	

NOTE: Germline mutation was also found in *A20*, *ABIN-1*, and *ABIN2*, but are not included in this table. Data with significance ($P < 0.05$) is boldface.

[a]Log-rank test.

[b]Cases with *A20* somatic mutations were excluded from the analysis so as to avoid confounding.

[c]Chromosome translocation involving the *BCL2*, *BCL6*, or *MYC* gene loci.

made several important and novel observations in this study. First, we have shown that *A20*-inactivating mutations and *CARD11*-activating mutations were frequent events in gastrointestinal DLBCL. Second, we have shown, for the first time, that ABIN-1 and ABIN-2, which are the adaptors of the A20 inhibitory complex of the NF-κB activation pathway, are also recurrently targeted by inactivating mutations, and that *A20*, *ABIN-1*, *ABIN-2*, and *CARD11* somatic mutations are almost mutually exclusive. Finally, among *A20*, *ABIN-1*, *ABIN-2*, and

Published OnlineFirst January 25, 2011; DOI:10.1158/1078-0432.CCR-10-1859

Table 2. The multivariate analysis of prognostic factors by Cox proportional hazards regression

	Prognostic variable[a]	Coefficient	SE	Relative risk	*P*
Overall survival	*A20* somatic mutation	1.740	0.648	5.697	0.007
Event-free survival	*A20* somatic mutation	1.414	0.613	4.112	0.021

[a]The prognostic variables that were included in the multivariate analysis are those with $P \leq 0.1$ by univariate analysis.

CARD11 genetic abnormalities, the *A20* somatic mutation was significantly and independently associated with both OS and EFS.

In line with previous findings (14, 15), we have also found frequent *CARD11* somatic mutations in gastrointestinal DLBCL, and all of these mutations were observed to cause missense changes. Intriguingly, among the 26 mutations that have been reported so far, only 1 mutation was recurrent, which was seen in 2 cases (Fig. 1A). Nonetheless, all CARD11 mutants were much more potent in NF-κB activation than the wild-type in the absence of any immune receptor stimulation, suggesting that these mutations may cause constitutive NF-κB activation.

A20, which is a target of the NF-κB transcription factor, attenuates NF-κB activities by inactivating several proteins that are critical to NF-κB signaling, such as RIP1/2, TRAF6, NEMO, and TAK1 (17–19). A20 can specifically remove the K63-linked ubiquitin chain that is crucial to protein function, and this is essentially mediated by the N-terminal OTU domain that belongs to the family of deubiquitinating cysteine proteases (25, 38). Additionally, A20 catalyzes the K48-linked polyubiquitin that targets proteins for proteasome degradation, and this is mediated by the C-terminal zinc finger (ZF) domains that possess E3 ligase activity (25, 38). In line with previous findings (15, 16, 22–24), the majority (79%) of the somatic mutations that have been seen in gastrointestinal DLBCL are insertion, deletion, nonsense, or splicing site mutations, all of which are predicted to produce truncated proteins that impair A20 function (Fig. 2B). Of the remaining 3 somatic missense mutations, 2 occurred within the known functional domain (1 in OTU and 1 in ZF) and the third between the third and fourth ZF domains. These mutations may also impair A20 function, although they have yet to be tested.

A20 does not directly recognize its substrates; this is mediated by A20 adaptor molecules, such as ABIN-1/2/3, TAX1BP1, Itch, and RNF11 (25). In this study, we have shown, for the first time, that *ABIN-1* and *ABIN-2* are also targeted by somatic mutations and that all of the identified somatic mutations could impair their respective functions. Of the 3 cases with *ABIN-1* somatic mutation, 2 exhibited frameshift mutations that predicted truncated products that lacked AHD1, UBAN, and NBD, which are critical to the binding of A20, ubiquitin, and NEMO, respectively (36). The deletion of these critical protein interaction domains is known to abolish the NF-κB inhibitory capacity of ABIN-1 (39–41). The remaining ABIN-1 E476K somatic mutation occurred within the highly conserved DFxxER motif of AHD2 (41). As shown in our NF-κB reporter assay, the single amino acid substitution (E476K) caused by a somatic point mutation was sufficient to completely abolish the NF-κB inhibitory function of the wild-type ABIN-1. The importance of this amino acid was also shown by the functional characterization of a double mutant (ER476-7AA) in a previous study (41). Similarly, the recurrent ABIN-2 E255K somatic mutation was also observed to occur at a highly conserved residue of AHD1, which is critical to the binding of A20 (42). Although this mutant did not exhibit unequivocal evidence of impaired NF-κB inhibition by reporter assays, immunoprecipitation clearly shows its defect in binding to A20. Thus, in essence, the somatic

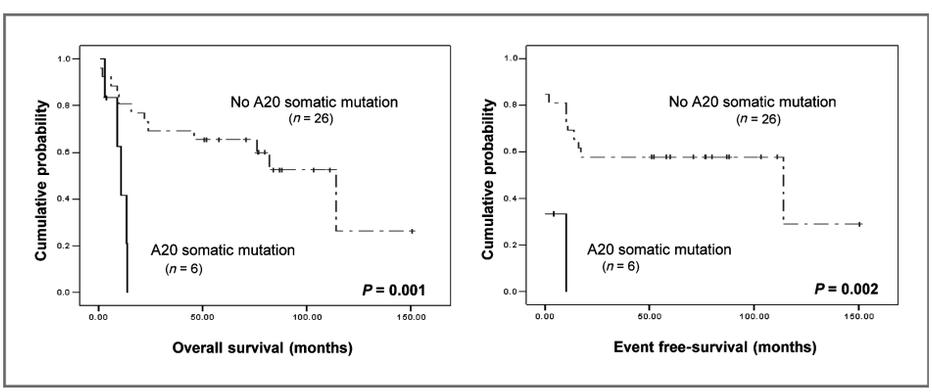

Figure 4. The impact of *A20* somatic mutation on the survival of patients with gastrointestinal DLBCL. Only 32 cases of gastrointestinal DLBCL treated with an anthracycline containing therapy were included in survival analysis. Among these cases, *A20* somatic mutations are significantly associated with both poor overall and EFS. A single germline mutation was also found in *A20*, but not included in this survival analysis.

Published OnlineFirst January 25, 2011; DOI:10.1158/1078-0432.CCR-10-1859

mutations that are seen in *ABIN-1* and *ABIN-2* could impair, if not completely abolish, their NF-κB inhibitory function.

Interestingly, *CARD11*, *A20*, *ABIN-1*, and *ABIN-2* somatic mutations were almost mutually exclusive, wherein only 1 of the 21 positive cases exhibited concurrent mutations that involved 2 or more of these genes. Given that all of these protein products commonly regulate the NF-κB activation pathway, it is conceivable that it might be unnecessary for tumor cells to acquire genetic abnormalities that affect more than one molecule in the same molecular pathway. Interestingly, among these abnormalities, the *A20* somatic mutation was significantly and independently associated with poor OS and EFS. In view of the fact that ABC-DLBCLs are associated with both *A20* mutations and poor clinical outcome (15, 16), further study is required to address whether the prognostic value of *A20* somatic mutation is totally independent of its association with the ABC subtype. There was no association between *A20* deletion, *CARD11*, *ABIN-1*, and *ABIN-2* somatic mutation and patients' survival. However, it should be noted that the number of cases with these abnormalities, particularly *ABIN-1* and *ABIN-2* somatic mutation, is small, not permitting a reliable survival analysis. In addition, the capacity of ABIN-1, most likely ABIN-2, in NF-κB inhibition is not as strong as A20 (43).

Germline mutation in the *A20*, *ABIN-1*, and *ABIN-2* genes is another interesting finding in this study. All of these germline mutations cause amino acid changes and have not been reported in the current SNP databases. It remains to be investigated whether these germline mutations are functional. By NF-κB reporter assay, the ABIN-1 and ABIN-2 germline mutants did not show apparent abnormalities in comparison with the wild-type. However, the reporter assay may not be an efficient approach to detecting the potential functional abnormalities of these missense mutations. For example, the ABIN-2 E255K somatic mutant, which had a major defect in its A20 binding, but showed no apparent defect by the reporter assay. The function of A20, ABIN-1, and ABIN-2 and their interacting proteins are not yet fully characterized. At this time, it is not possible to further test these germline mutants by using conventional immunoprecipitation experiments. Nonetheless, the recent finding of the association of the *A20* and *ABIN-2* gene polymorphisms to several chronic inflammatory disorders, including rheumatoid arthritis and systemic lupus erythematosus (17, 44–51), highlights the importance of the functional characterization of these germline mutations in the future.

The NF-κB activation pathway is governed and regulated by many positive and negative regulators. In addition to the aforementioned *CARD11*, *A20*, *ABIN-1*, and *ABIN-2* gene mutations, mutations in *TNFSF11A* (*RANK*), *TRAF5*, *TRAF2*, and *MAP3K7* (*TAK1*), although generally at a low frequency, have also been reported in nodal DLBCL (15). Recently, Davis and colleagues reported the frequent activating mutation (16%) of CD79B in DLBCL (52). Studies of MM have shown inactivating mutations in the NF-κB–negative regulators, including *TRAF2*, *TRAF3*, *CYLD*, and *API1*/*API2*, and activating mutations in the NF-κB–positive regulators, including *NF-κB1*, *NF-κB2*, *CD40*, *LTBR*, *TACI*, and *NIK* (10, 11). The full scale of NF-κB regulator genetic abnormality in DLBCL and in reference to disease prognosis and treatment prediction remains to be investigated.

Nonetheless, the finding of a significant association between NF-κB pathway gene abnormalities and poor prognosis in gastrointestinal DLBCL may have important implications to patient management. Previous studies have shown that the NF-κB pathway gene mutations that are seen in DLBCL are more frequent in the ABC subtype than the germinal center B-cell like (GCB) subtype (14–16). In line with this, we have also found that *A20*, *ABIN-1*, and *ABIN-2*, but not *CARD11* somatic mutation, were more frequent in non-GC than in GC-DLBCL, as defined by the immunohistochemistry algorithm of Hans and colleagues (31). ABC-DLBCL is characterized by constitutive NF-κB activation (13) and exhibits a much poorer survival than GCB-DLBCL, regardless of being treated with CHOP or R-CHOP (53). In light of the recent advances in the development of NF-κB inhibitors and their potential application in cancer therapies, a comprehensive characterization of NF-κB regulator gene abnormalities and their prognostic value in DLBCL will not only benefit current patient care, and also provide a basis for the design of future therapeutic strategies that incorporate NF-κB inhibitors.

Disclosure of Potential Conflicts of Interest

No potential conflicts of interest were disclosed.

Author contributions

G. Dong, E. Chanudet, N. Zeng, A. Appert performed key experiments, analyzed data, and prepared the figures; R.A. Hamoudi assisted in DNA sequencing and statistical analyses; A.J. Watkins reviewed histology and assisted in microdissection; H. Ye and H. Liu assisted in interphase FISH detection of chromosome translocation. Y-W. Chen, W-Y. Au, Z. Gao, S-S. Chuang, G. Srivastava contributed majority of the cases for the study; M-Q. Du designed, coordinated the study, and wrote the manuscript.

Acknowledgments

We thank Dr. Ian McFarlane (The Microarray CoreLab, National Institute of Health Research, Cambridge Comprehensive Biomedical Research Centre) for his help in DNA sequencing, and Drs. Georg Lenz and Louis Staudt for providing CARD11 expression construct.

Grant Support

The research in M-Q. Du laboratory was supported by grants from Leukemia and Lymphoma Research, UK; the Elimination of Leukemia Fund, UK; the Lady Tata Memorial Trust and the Kay Kendal Leukemia Fund, UK. G. Dong was supported by a fellowship from the China Scholarship Council.

The costs of publication of this article were defrayed in part by the payment of page charges. This article must therefore be hereby marked *advertisement* in accordance with 18 U.S.C. Section 1734 solely to indicate this fact.

Received July 12, 2010; revised November 17, 2010; accepted November 29, 2010; published OnlineFirst January 25, 2011.

Published OnlineFirst January 25, 2011; DOI:10.1158/1078-0432.CCR-10-1859

References

1. Du MQ. MALT lymphoma: recent advances in aetiology and molecular genetics. J Clin Exp Hematop 2007;47:31–42.
2. Davis RE, Brown KD, Siebenlist U, Staudt LM. Constitutive nuclear factor kappaB activity is required for survival of activated B cell-like diffuse large B cell lymphoma cells. J Exp Med 2001;194:1861–74.
3. Feuerhake F, Kutok JL, Monti S, Chen W, LaCasce AS, Cattoretti G, et al. NFkappaB activity, function, and target-gene signatures in primary mediastinal large B-cell lymphoma and diffuse large B-cell lymphoma subtypes. Blood 2005;106:1392–9.
4. Rosenwald A, Wright G, Leroy K, Yu X, Gaulard P, Gascoyne RD, et al. Molecular diagnosis of primary mediastinal B cell lymphoma identifies a clinically favorable subgroup of diffuse large B cell lymphoma related to Hodgkin lymphoma. J Exp Med 2003;198:851–62.
5. Savage KJ, Monti S, Kutok JL, Cattoretti G, Neuberg D, De Leval L, et al. The molecular signature of mediastinal large B-cell lymphoma differs from that of other diffuse large B-cell lymphomas and shares features with classical Hodgkin lymphoma. Blood 2003;102:3871–9.
6. Rajkumar SV, Richardson PG, Hideshima T, Anderson KC. Proteasome inhibition as a novel therapeutic target in human cancer. J Clin Oncol 2005;23:630–9.
7. Jost PJ, Ruland J. Aberrant NF-kappaB signaling in lymphoma: mechanisms, consequences, and therapeutic implications. Blood 2007;109:2700–7.
8. Chanudet E, Ye H, Ferry J, Bacon CM, Adam P, Müller-Hermelink HK, et al. A20 deletion is associated with copy number gain at the TNFA/B/C locus and occurs preferentially in translocation-negative MALT lymphoma of the ocular adnexa and salivary glands. J Pathol 2009;217:420–30.
9. Chanudet E, Huang Y, Ichimura K, Dong G, Hamoudi RA, Radford J, et al. A20 is targeted by promoter methylation, deletion and inactivating mutation in MALT lymphoma. Leukemia 2010;24:483–7.
10. Keats JJ, Fonseca R, Chesi M, Schop R, Baker A, Chng WJ, et al. Promiscuous mutations activate the noncanonical NF-kappaB pathway in multiple myeloma. Cancer Cell 2007;12:131–44.
11. Annunziata CM, Davis RE, Demchenko Y, Bellamy W, Gabrea A, Zhan F, et al. Frequent engagement of the classical and alternative NF-kappaB pathways by diverse genetic abnormalities in multiple myeloma. Cancer Cell 2007;12:115–30.
12. Thome M, Weil R. Post-translational modifications regulate distinct functions of CARMA1 and BCL10. Trends Immunol 2007;28:281–8.
13. Ngo VN, Davis RE, Lamy L, Yu X, Zhao H, Lenz G, et al. A loss-of-function RNA interference screen for molecular targets in cancer. Nature 2006;441:106–10.
14. Lenz G, Davis RE, Ngo VN, Lam L, George TC, Wright GW, et al. Oncogenic CARD11 mutations in human diffuse large B cell lymphoma. Science 2008;319:1676–9.
15. Compagno M, Lim WK, Grunn A, Nandula SV, Brahmachary M, Shen Q, et al. Mutations of multiple genes cause deregulation of NF-kappaB in diffuse large B-cell lymphoma. Nature 2009;459:717–21.
16. Honma K, Tsuzuki S, Nakagawa M, Tagawa H, Nakamura S, Morishima Y, et al. TNFAIP3/A20 functions as a novel tumor suppressor gene in several subtypes of non-Hodgkin lymphomas. Blood 2009;114:2467–75.
17. Vereecke L, Beyaert R, Van Loo G. The ubiquitin-editing enzyme A20 (TNFAIP3) is a central regulator of immunopathology. Trends Immunol 2009;30:383–91.
18. Boone DL, Turer EE, Lee EG, Ahmad RC, Wheeler MT, Tsui C, et al. The ubiquitin-modifying enzyme A20 is required for termination of Toll-like receptor responses. Nat Immunol 2004;5:1052–60.
19. Thome M, Tschopp J. TCR-induced NF-kappaB activation: a crucial role for Carma1, Bcl10 and MALT1. Trends Immunol 2003;24:419–24.
20. Kim WS, Honma K, Karnan S, Tagawa H, Kim YD, Oh YL, et al. Genome-wide array-based comparative genomic hybridization of ocular marginal zone B cell lymphoma: comparison with pulmonary and nodal marginal zone B cell lymphoma. Genes Chromosomes Cancer 2007;46:776–83.
21. Honma K, Tsuzuki S, Nakagawa M, Karnan S, Aizawa Y, Kim WS, et al. TNFAIP3 is the target gene of chromosome band 6q23.3-q24.1 loss in ocular adnexal marginal zone B cell lymphoma. Genes Chromosomes Cancer 2008;47:1–7.
22. Novak U, Rinaldi A, Kwee I, Nandula SV, Rancoita PM, Compagno M, et al. The NF-{kappa}B negative regulator TNFAIP3 (A20) is inactivated by somatic mutations and genomic deletions in marginal zone lymphomas. Blood 2009;113:4918–21.
23. Kato M, Sanada M, Kato I, Sato Y, Takita J, Takeuchi K, et al. Frequent inactivation of A20 in B-cell lymphomas. Nature 2009;459:712–6.
24. Schmitz R, Hansmann ML, Bohle V, Martin-Subero JI, Hartmann S, Mechtersheimer G, et al. TNFAIP3 (A20) is a tumor suppressor gene in Hodgkin lymphoma and primary mediastinal B cell lymphoma. J Exp Med 2009;206:981–9.
25. Coornaert B, Carpentier I, Beyaert R. A20: central gatekeeper in inflammation and immunity. J Biol Chem 2009;284:8217–21.
26. Ferreri AJ, Montalban C. Primary diffuse large B-cell lymphoma of the stomach. Crit Rev Oncol Hematol 2007;63:65–71.
27. Chen LT, Lin JT, Tai JJ, Chen GH, Yeh HZ, Yang SS, et al. Long-term results of anti-Helicobacter pylori therapy in early-stage gastric high-grade transformed MALT lymphoma. J Natl Cancer Inst 2005;97:1345–53.
28. Raderer M, Paul dB. Role of chemotherapy in gastric MALT lymphoma, diffuse large B-cell lymphoma and other lymphomas. Best Pract Res Clin Gastroenterol 2010;24:19–26.
29. Hu XT, Chen YW, Liang AC, Au WY, Wong KY, Wan TS, et al. CD44 activation in mature B-cell malignancies by a novel recurrent IGH translocation. Blood 2010;115:2458–61.
30. Chuang SS, Ye H, Yang SF, Huang WT, Chen HK, Hsieh PP, et al. Perforation predicts poor prognosis in patients with primary intestinal diffuse large B-cell lymphoma. Histopathology 2008;53:432–40.
31. Hans CP, Weisenburger DD, Greiner TC, Gascoyne RD, Delabie J, Ott G, et al. Confirmation of the molecular classification of diffuse large B-cell lymphoma by immunohistochemistry using a tissue microarray. Blood 2004;103:275–82.
32. Pan LX, Diss TC, Peng HZ, Isaacson PG. Clonality analysis of defined B-cell populations in archival tissue sections using microdissection and the polymerase chain reaction. Histopathology 1994;24:323–7.
33. Liu H, Bench AJ, Bacon CM, Payne K, Huang Y, Scott MA, et al. A practical strategy for the routine use of BIOMED-2 PCR assays for detection of B- and T-cell clonality in diagnostic haematopathology. Br J Haematol 2007;138:31–43.
34. Nakamura S, Ye H, Bacon CM, Goatly A, Liu H, Banham AH, et al. Clinical impact of genetic aberrations in gastric MALT lymphoma: a comprehensive analysis using interphase fluorescence in situ hybridisation. Gut 2007;56:1358–63.
35. Hamoudi RA, Appert A, Ye H, Ruskone-Fourmestraux A, Streubel B, Chott A, et al. Differential expression of NF-kappaB target genes in MALT lymphoma with and without chromosome translocation: insights into molecular mechanism. Leukemia 2010;24:1487–97.
36. Verstrepen L, Carpentier I, Verhelst K, Beyaert R. ABINs: A20 binding inhibitors of NF-kappa B and apoptosis signaling. Biochem Pharmacol 2009;78:105–14.
37. Lang V, Symons A, Watton SJ, Janzen J, Soneji Y, Beinke S, et al. ABIN-2 forms a ternary complex with TPL-2 and NF-kappa B1 p105 and is essential for TPL-2 protein stability. Mol Cell Biol 2004;24:5235–48.
38. Sun SC. Deubiquitylation and regulation of the immune response. Nat Rev Immunol 2008;8:501–11.
39. Heyninck K, Kreike MM, Beyaert R. Structure-function analysis of the A20-binding inhibitor of NF-kappa B activation, ABIN-1. FEBS Lett 2003;536:135–40.
40. Mauro C, Pacifico F, Lavorgna A, Mellone S, Iannetti A, Acquaviva R, et al. ABIN-1 binds to NEMO/IKKgamma and co-operates with A20 in inhibiting NF-kappaB. J Biol Chem 2006;281:18482–8.
41. Wagner S, Carpentier I, Rogov V, Kreike M, Ikeda F, Löhr F, et al. Ubiquitin binding mediates the NF-kappaB inhibitory potential of ABIN proteins. Oncogene 2008;27:3739–45.
42. Van Huffel S, Delaei F, Heyninck K, De Valck D, Beyaert R. Identification of a novel A20-binding inhibitor of nuclear factor-kappa B activation termed ABIN-2. J Biol Chem 2001;276:30216–23.

43. Oshima S, Turer EE, Callahan JA, Chai S, Advincula R, Barrera J, et al. ABIN-1 is a ubiquitin sensor that restricts cell death and sustains embryonic development. Nature 2009;457:906–9.

44. Graham RR, Cotsapas C, Davies L, Hackett R, Lessard CJ, Leon JM, et al. Genetic variants near TNFAIP3 on 6q23 are associated with systemic lupus erythematosus. Nat Genet 2008;40:1059–61.

45. Dieguez-Gonzalez R, Calaza M, Perez-Pampin E, Balsa A, Blanco FJ, Cañete JD, et al. Analysis of TNFAIP3, a feedback inhibitor of nuclear factor-kappaB and the neighbor intergenic 6q23 region in rheumatoid arthritis susceptibility. Arthritis Res Ther 2009;11:R42.

46. Plenge RM, Cotsapas C, Davies L, Price AL, de Bakker PI, Maller J, et al. Two independent alleles at 6q23 associated with risk of rheumatoid arthritis. Nat Genet 2007;39:1477–82.

47. Kawasaki A, Ito S, Furukawa H, Hayashi T, Goto D, Matsumoto I, et al. Association of TNFAIP3 interacting protein 1, TNIP1 with systemic lupus erythematosus in a Japanese population: a case-control association study. Arthritis Res Ther 2010;12:R174.

48. He CF, Liu YS, Cheng YL, Gao JP, Pan TM, Han JW, et al. TNIP1, SLC15A4, ETS1, RasGRP3 and IKZF1 are associated with clinical features of systemic lupus erythematosus in a Chinese Han population. Lupus 2010;19:1181–6.

49. Han JW, Zheng HF, Cui Y, Sun LD, Ye DQ, Hu Z, et al. Genome-wide association study in a Chinese Han population identifies nine new susceptibility loci for systemic lupus erythematosus. Nat Genet 2009;41:1234–7.

50. Gateva V, Sandling JK, Hom G, Taylor KE, Chung SA, Sun X, et al. A large-scale replication study identifies TNIP1, PRDM1, JAZF1, UHRF1BP1 and IL10 as risk loci for systemic lupus erythematosus. Nat Genet 2009;41:1228–33.

51. Nair RP, Duffin KC, Helms C, Ding J, Stuart PE, Goldgar D , et al. Genome-wide scan reveals association of psoriasis with IL-23 and NF-kappaB pathways. Nat Genet 2009;41:199–204.

52. Davis RE, Ngo VN, Lenz G, Tolar P, Young RM, Romesser PB, et al. Chronic active B-cell-receptor signalling in diffuse large B-cell lymphoma. Nature 2010;463:88–92.

53. Lenz G, Staudt LM. Aggressive lymphomas. N Engl J Med 2010;362:1417–29.